Critical exponents of block-block mutual information in one-dimensional infinite lattice systems

Yan-Wei Dai,[1] Xi-Hao Chen,[2] Sam Young Cho,[1,3,*] and Huan-Qiang Zhou[1,3]
[1]*Centre for Modern Physics, Chongqing University, Chongqing 400044, China*
[2]*Research Institute for New Materials and Technology, Chongqing University of Arts and Sciences, Chongqing 402160, China*
[3]*Department of Physics, Chongqing University, Chongqing 400044, China*

(Received 5 September 2020; revised 16 August 2021; accepted 4 October 2021; published 29 October 2021)

We study the mutual information between two lattice blocks in terms of von Neumann entropies for one-dimensional infinite lattice systems. Quantum q-state Potts model and transverse-field spin-1/2 XY model are considered numerically by using the infinite matrix product state approach. As a system parameter varies, block-block mutual information exhibit singular behaviors that enable us to identify the critical points for the quantum phase transitions. As happens with von Neumann entanglement entropy of single block, at critical points, block-block mutual information for two adjacent blocks show a logarithmic leading behavior with increasing the size of the blocks, which yields the central charge c of the underlying conformal field theory, as it should be. It seems that two disjoint blocks show a similar logarithmic growth of the mutual information as a characteristic property of critical systems but the proportional coefficients of the logarithmic term are very different from the central charges. As the separation between the two lattice blocks increases, the mutual information reveals a consistent power-law decaying behavior for various truncation dimensions and lattice-block sizes. The critical exponent of block-block mutual information in the thermodynamic limit is estimated by extrapolating the exponents of power-law decaying regions for finite truncation dimensions. For a given lattice-block size ℓ, the critical exponents for the same universality classes seem to have very close values each other. Whereas the critical exponents have different values to a degree of distinction for the different universality classes. As the lattice-block size becomes bigger, the critical exponent becomes smaller. We discuss a relation between the exponents of block-block mutual information and correlation with the Shatten one-norm of block-block correlation.

DOI: 10.1103/PhysRevE.104.044137

I. INTRODUCTION

As an information of one system about another, correlations quantify a relationship or connection between them. Correlations have long been a central theme of physical quantities in characterizing a unique property of strongly correlated systems in condensed matters. Conventional two-point spatial correlation functions have been studied and their scaling behaviors have been then used to characterize quantum phases of many-body systems [1,2]. Recently much attention has been drawn to quantum entanglement that can quantify unique correlations present in quantum states. Such as entanglement entropy, concurrence, and Rényi entropy, quantum information theoretical tools have been shown to be useful to investigate quantum critical points and different phases in strongly correlated systems [3].

Similar to conventional two-point correlations, in general, a correlation between two blocks embedded in a large system may also be considered to study a characteristic behavior of the system. For a chosen size of blocks, block-block correlations can be in principle from either classical or quantum origin. Not due to entanglement, nontrivial quantum correlations can exist [4]. Although correlations can be induced from such different origins and specific dominant correlations are not known to characterize the system, the mutual information can be used to measure all kinds of correlations of one block about the other, i.e., the total amount of classical and quantum correlations between two blocks [5–8]. In terms of the von Neumann entropies, the mutual information $I(A:B)$ between two lattice blocks A and B (see Fig. 1) can be defined as

$$I(A:B) = S(A) + S(B) - S(A \cup B), \tag{1}$$

where $S(\alpha) = -\mathrm{Tr}\rho_\alpha \log_2 \rho_\alpha$ is the von Neumann entropy for the lattice blocks with $\alpha \in \{A, B, A \cup B\}$. To calculate the mutual information between two lattice blocks in the system, the density matrix ρ_α can be expressed in terms of expectation values of operators in the blocks. The elements of the density matrix have the form of generalized correlations functions and contain, by definition, all block-site correlations. The block-block mutual information in terms of the von Neumann entropy consists of a weighted average of generalized correlation functions and, in fact, measures the strength of the overall correlation between two blocks of sizes ℓ_A and ℓ_B. This implies that without knowing a dominant correlation between blocks in the system and its corresponding operator, the mutual information can capture a characteristic property of the system even if hidden or exotic correlations present. The two-point pairwise mutual information has then been used to study quantum phase transitions [9–21]. A recent study shows

*sycho@cqu.edu.cn

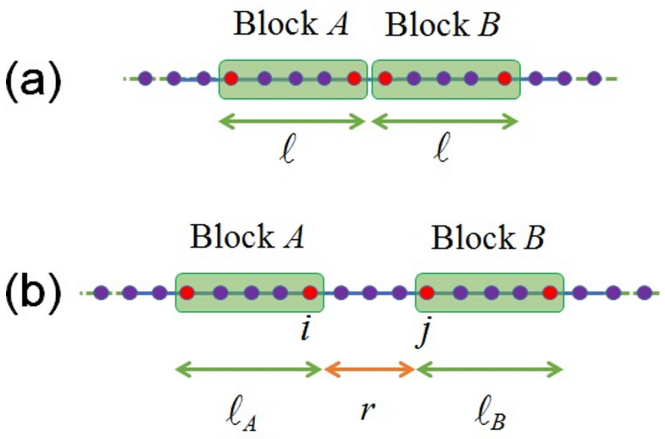

FIG. 1. Two (a) adjacent and (b) disjoint lattice blocks A and B in one-dimensional infinite lattice systems. The block sizes are denoted by l_A and l_B, respectively. The size of the blocks l_A and l_B are denoted by the number of sites inside the blocks, respectively. $r = |i - j|$ is the lattice distance between two blocks.

that similar to two-point spatial correlations, two-point pairwise mutual information can characterize one-dimensional quantum critical systems by using its critical exponent [21]. In contrast with two-point pairwise mutual information, criticality of systems has also been studied by considering the mutual information between the two lattice blocks for bipartite systems [17–20].

To more deeply understand mutual information in critical systems, it would be interesting to study mutual information between lattice blocks embedded in infinite lattice systems in Fig. 1. Two consecutive subchains in one-dimensional spin models [e.g., see Fig. 1(a)] exhibit a logarithmical growth of the entanglement with respect to the size of subchains at critical points. Compared with two such consecutive subchains, no correlation between disjoint lattice blocks [e.g., see Fig. 1(b)] is expected for a large separation at a transition. Then it would be interesting to study (i) how this correlation between disjoint lattice blocks behaves with their separation r, i.e., how it scales, at a quantum phase transition and also (ii) how the size ℓ of the lattice blocks affects the scaling. Such blocks in critical systems [22–42] have been considered to investigate the entanglement entropy, the entanglement negativity, and the mutual information. Specifically, for a quantum formal field theory, Furukawa *et al.* [24] predicted that the von Neumann entanglement entropy of two lattice blocks $A = [x_1, x_2]$ and $B = [x_3, x_4]$ in an infinite lattice is given by

$$S(A \cup B) = S^{\mathrm{CC}}_{A\cup B} - \lim_{n\to 1} \frac{1}{n-1} \log F_n(x), \tag{2a}$$

with the prediction of Calabrese and Cardy (CC) [24,25]

$$S^{\mathrm{CC}}_{A\cup B} = \frac{c}{3} \log\left(\frac{x_{21}x_{32}x_{43}x_{41}}{x_{31}x_{42}}\right) + 2s_1, \tag{2b}$$

where c is the central charge of the conformal field theory, $x_{ij} \equiv x_i - x_j$ and $x = (x_{32}x_{41})/(x_{31}x_{42})$. The constant $2s_1$ is determined under the condition $S^{\mathrm{CC}}_{A\cup B} \to S(A) + S(B)$ in the limit $x_{21}, x_{43} \ll x_{31}, x_{42}$. The function $F_n(x)$ depends on the details of the model and thus it should be calculated case by case [26,40]. The scaling functions of the von Neumann entanglement entropy (mutual information) have been studied for the Ising model [31,33,41] and for the spin-1/2 XXZ model [24,41]. As is shown in Eqs. (2a) and (2b), actually, it has been found that studying the scaling functions is a very nontrivial task because the scaling functions depend not only on the central charge but also on more universal information of the conformal field theory [23,24,26].

In this paper we investigate the block-block mutual information between two lattice blocks in infinite-lattice systems by using the infinite matrix product state (iMPS) representation with the infinite time-evolving block decimation (iTEBD) method [43–45]. To consider various universality classes at critical points, we consider quantum q-state Potts model and transverse-field spin-1/2 XY model, and calculate the von Neuman mutual information for various sizes of lattice blocks. We demonstrate that the block-block mutual information can be a useful probe for detecting quantum phase transition. The scaling of the block-block mutual information is studied at the critical point in the thermodynamic limit. The numerical results show that similar to conventional two-point correlations, block-block information exhibits power-law decaying behaviors. We find that as the size of lattice block ℓ increases, the critical exponent decreases. The scaling behaviors of ground-state block-block mutual information are discussed in associations with a characterization of critical systems. To study a connection between block-block mutual information and correlation, as the upper bound of block-block correlations, the Shatten-one norm of the correlation density matrix is calculated. The Shatten-one norm shows a power-law decay to zero at the critical systems for the both quantum q-state Potts model and transverse-field spin-1/2 XY model with the truncation dimension $\chi = 150$. Similar to the critical exponents of the mutual information, it is found that the larger the size of lattice block ℓ becomes, the smaller the critical exponent $\eta_{\chi=150}(\ell)$ of the Shatton-one norm becomes. Comparison to the exponent of the mutual information $\eta^I_{\chi=150}(\ell)$ shows that regardless of the universality classes and the size of the blocks, the critical exponents of the mutual information and the Shatton-one norm seem to relate each other by $\eta^I_{\chi=150}(\ell) \sim 2\eta_{\chi=150}(\ell)$.

This paper is organized as follows.

In Sec. IV B, we briefly introduce one-dimensional q-state quantum Potts model and numerical iMPS approach. A singular behavior of block-block mutual information appears to identify a quantum phase transition. In Sec. III, for the both adjacent and disjoint blocks at the critical points, the block-block mutual information shows a logarithmic scaling behavior. In Sec. IV, block-block mutual information is shown to decrease as the separation of blocks increases. The power-law decaying behaviors and the critical exponents are discussed in the thermodynamic limit for the transverse field spin-1/2XY model as well as the q-state quantum Potts model for various sizes of lattice blocks. In Sec. V, we calculate the Shatton one-norm of the correlation density matrix as the upper bound of the block-block correlation functions. The relationship between the exponents of the mutual information and the Shatton one-norm is discussed for the truncation dimension $\chi = 150$.

Summary of this work is given in Sec. VI. In Appendix A, we present the mutual information of the two adjacent blocks

as a function of the system parameter in the one-dimensional quantum q-state Potts model. Appendix B devotes to the detailed discussions on central charges from the block entanglement entropies in the one-dimensional quantum q-state Potts model. Appendix C shows the detailed scaling behaviors of block-block mutual information for the transverse-field spin-1/2 XY model. In Appendix D, the block-block mutual information is calculated in the ordered and the disordered phases for the q-state quantum Potts model. It is shown that the block-block mutual information decays to zero exponentially in the both ordered and disordered phases.

II. ONE-DIMENSIONAL q-STATE QUANTUM POTTS MODEL AND MUTUAL INFORMATION

We consider q-state quantum Potts model [46] with the nearest-neighbor interaction in a transverse magnetic field λ. The Hamiltonian can be written as

$$H = -\sum_{i=1}^{\infty}\left[\sum_{p=1}^{q-1} M_{x,p}^{i} M_{x,q-p}^{i+1} + \lambda M_{z}^{i}\right], \tag{3}$$

where $M_{x,p} = (M_{x,1})^{p}$ and the Potts spin matrices $M_{x/z}$ are given as

$$M_{x,1} = \begin{pmatrix} 0 & I_{q-1} \\ 1 & 0 \end{pmatrix} \text{and} \, M_{z} = \begin{pmatrix} q-1 & 0 \\ 0 & -I_{q-1} \end{pmatrix}, \tag{4}$$

with the $(q-1)\times(q-1)$ identity matrix I_{q-1}. Due to the spontaneous symmetry breaking with the symmetry group Z_q, q-degenerate ground states emerge in the broken symmetry phases. It is known that a (dis-)continuous quantum phase transition occurs for $(q > 4)$ $q \leqslant 4$ in the one-dimensional quantum q-state Potts model [47–50].

To consider an one-dimensional infinite lattice of the system, we employ a wave function $|\psi\rangle$ of Hamiltonian in the iMPS representation. The iTEBD algorithm with the second-order Trotter decomposition leads to a numerical ground state $|\psi_g\rangle$ in the iMPS representation. As the initially chosen state approaches to a ground state, according to a power law, the time step is decreased from an initial time step $dt = 0.1$ to $dt = 10^{-6}$. Then numerical iMPS wave functions for ground states are obtained for the truncation dimensions between $\chi = 20$ and $\chi = 150$. Actually, in the broken-symmetry phases, randomly chosen several initial states can reach different orthogonal ground states that are degenerate ground states for a spontaneous symmetry breaking and can be distinguished by using quantum fidelity [50,51]. Our iMPS approach gives the full description of the ground state in a pure state by the iMPS ground-state wave function $|\psi_g\rangle$. The reduced density matrices $\rho_{A/B}$ are obtained from the full density matrix $\rho = |\psi_g\rangle\langle\psi_g|$ by tracing out the degrees of freedom of the rest of the lattice block A or B, i.e., $\rho_{A/B} = \mathrm{Tr}_{A^c/B^c}\,\rho$. Thus, also $\rho_{A\cup B} = \mathrm{Tr}_{(A\cup B)^c}\,\rho$.

Based on our iMPS ground-state wave functions, we first consider the mutual information $I_q(A:B)$ between the two lattice blocks of ℓ contiguous sites, i.e., $\ell_A = \ell_B = \ell$, with the lattice distance $r = 2$ and 3 in Fig. 1(b). For the broken symmetry phases, i.e., $\lambda < \lambda_c$, if one chooses a random state as a reference state, one can detect q degenerate ground states by using the quantum fidelity [50]. All q degenerate ground states give the same block-block mutual information.

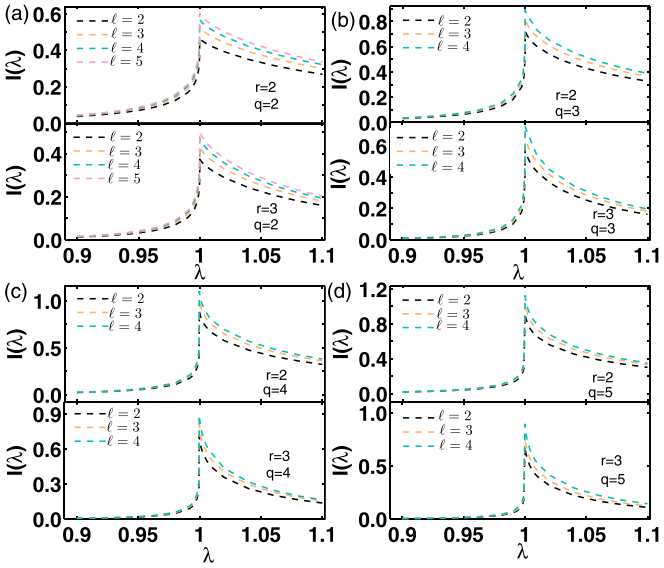

FIG. 2. Mutual information $I_q(\lambda)$ of two disjoint lattice blocks with the lattice distances $r = 2$ and 3 as a function of the transverse field λ for one-dimensional q-state quantum Potts model with various sizes of lattice blocks ℓ.

In Figs. 2(a) $q = 2$, 2(b) $q = 3$, 2(c) $q = 4$, and 2(d) $q = 5$, we plot the mutual information $I_q(\lambda)$ as a function of the transverse field λ for various sizes of lattice blocks ℓ. One can notice that compared for smaller lattice-block size, the block-block mutual information for bigger lattice-block size has a bigger value. Furthermore, all the block-block mutual information exhibit a singular behavior for various sizes of lattice blocks ℓ. The singular points correspond to the phase transition points $\lambda_c = 1$. The overall features of the block-block mutual information for $r = 3$ are similar to those for $r = 2$. Only the case $r = 2$ has a larger value than the case $r = 3$. Consequently, the block-block mutual information of the disjoint lattice blocks can detect quantum phase transition.

The disjoint lattice blocks of $r = 1$ in Fig. 1(b) is the very adjacent lattice blocks in Fig. 1(a). The block-block mutual information of the adjacent lattice blocks also exhibit overall similar features to those of the disjoint lattices-blocks for $r = 2$ and $r = 3$ (see Fig. 10 in Appendix A). Only the values of the mutual information for the adjacent lattice blocks $r = 1$ are larger than those for the disjoint lattice blocks for $r = 2$ and $r = 3$. This shows that as the lattice distance increases, the value of the block-block mutual information decreases. Note that all the block-block mutual information of the adjacent blocks exhibit similar singular behaviors to those of the disjoint blocks for various sizes of lattice blocks ℓ at the phase transition points $\lambda_c = 1$. Regardless of whether the adjacent or the disjoint lattice blocks, as a result, it is shown that the block-block mutual information can capture quantum phase transitions for the spontaneous symmetry breaking.

III. CENTRAL CHARGES AND QUANTUM MUTUAL INFORMATION

As was discussed in the previous section, the critical quantum Potts chains with $q = 2$, 3, and 4 for $\lambda = \lambda_c$ can be detected by using the mutual information $I_q(\lambda)$ between two lattice blocks. The universality classes of the critical quantum Potts chains can be identified by calculating the central charge c that is the main feature of conformal field theory. Actually, the von Neumann entanglement entropy of a block provides an accurate way of detecting the value of the central charge because the entropy turns out to be proportional to the logarithm of the size of block ℓ and the proportional coefficient, being generally universal, gives the central charge in conformal systems [25,52–59]:

$$S(\ell) = \frac{c}{3}\log_2 \ell + c', \tag{5}$$

where c' is a nonuniversal constant. To show that our iMPS approach is reliable, we presents the von Neumann entropy in Appendix B. Our numerical result shows such a logarithmic scaling of the von Neumann entropy for single lattice blocks in the one-dimensional q-state quantum Potts model and the estimates of the central charges are in excellent agreement with the exact values at the critical points (see Fig. 11 in Appendix B).

In contrast to the von Neumann entanglement entropy for single lattice blocks in Eq. (5), as was discussed in the Introduction, the von Neumann entanglement entropy for two lattice blocks was predicted to consist of the two contributions in Eqs. (2a) and (2b). One is proportional to the central charge predicted by Calabrese and Cardy [25]. The other is the characteristic function F_n that contains detailed information of conformal field theory beyond the central charge [22–24,26]. Thus, the explicit expression of the von Neumann entanglement entropy for two lattice blocks is unknown, so neither does the block-block mutual information know its explicit expression.

A. Mutual information of two adjacent blocks

To compare with the case of the disjoint blocks ($r > 1$) in Fig. 1(b) in our iMPS approach, let us first consider the mutual information $I(\ell)$ of the adjacent blocks in Fig. 1(a), i.e., the $r = 1$ case of the disjoint blocks in Fig. 1(b), on varying the sizes of lattice blocks ℓ. The mutual information $I(\ell)$ between the adjacent blocks is plotted as a function of the size of lattice blocks ℓ in Fig. 3 at the critical points. Similar to the von Neumann entanglement entropy in Eq. (5), the von Neumann mutual information $I(\ell)$ exhibits a logarithmic increment as the size of lattice block ℓ increases. For the Shannon mutual information with two blocks A and B of sizes ℓ and $L - \ell$, the similar logarithmic scaling behavior has been conjectured for periodic chains in the ground state in Refs. [17–19], i.e., $I_{sh}(\ell, L) = c/4 \ln[L/\pi \sin(\pi\ell/L)] + \gamma_I$ based on the Shanon entropy in the scaling regime ($\ell, L \gg 1$), where L is the system size and ℓ is the subsystem size, and γ_I is the nonuniversal constant. To clarify the logarithmic behaviors of our mutual information $I(A:B)$, thus we perform a numerical best fit

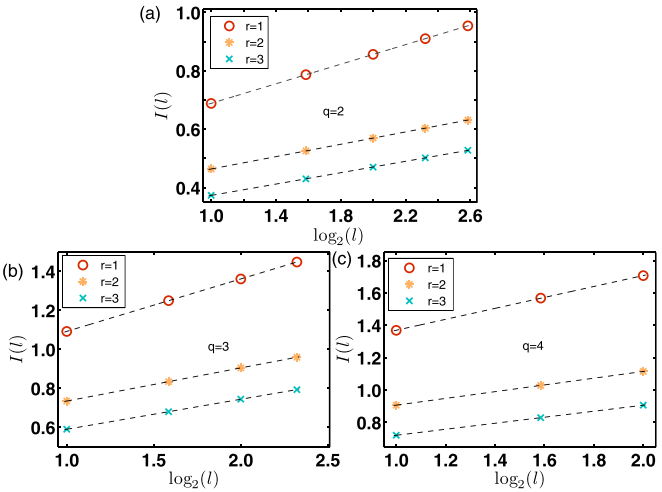

FIG. 3. Mutual information $I(\ell)$ for the lattice distance $r = 1$, 2, and 3 as a function of the size of lattice block $\ell_A = \ell_B = \ell$ at the critical point $\lambda = \lambda_c$ for the quantum Potts chains with (a) $q = 2$, (b) $q = 3$, and (c) $q = 4$. The lines are the numerical fitting functions $I_q(\ell) = a_q \log_2 \ell + b_q$ with the numerical coefficients a_q and b_q. The detailed discussions are in the text.

with the fitting function

$$I_q(\ell) = a_q \log_2 \ell + b_q, \tag{6}$$

where a_q and b_q are numerical coefficients. The numerical fitting coefficients with the fitting errors [60] are given as (i) $a_2 = 0.1676(7)$ and $b_2 = 0.521(1)$ for $q = 2$, (ii) $a_3 = 0.269(1)$ and $b_3 = 0.823(2)$ for $q = 3$, and (iii) $a_4 = 0.34(2)$ and $b_4 = 1.03(3)$ for $q = 4$. Actually, the coefficient of the logarithm in the entanglement entropy in Eq. (5) is dependent on the central charge c. For comparison with the entanglement entropy in Eq. (5), we then consider the coefficients $3a_q$, i.e., (i) $3a_2 = 0.503(2)$ for $q = 2$, (ii) $3a_3 = 0.808(4)$ for $q = 3$, and (iii) $3a_4 = 1.01(6)$ for $q = 4$. One can notice that if one assumes that similar to the entanglement entropy in Eq. (5), the proportional coefficient a_q corresponds to a central charge via $c_q = 3a_q$, then our results of the central charges c_q obtained from the mutual information $I(\ell)$ of the two adjacent blocks are very close to the exact results $c = 1/2$, $c = 4/5$, and $c = 1$ for $q = 2$, 3, and 4, respectively.

In Table I, the estimates of central charges c obtained from the mutual information $I(A:B)$ of the two adjacent blocks are summarized in comparison with those values from the von Neumann block entropy (Appendix B). This result shows that for two adjacent lattice blocks of critical one-

TABLE I. Numerical central charges c estimated from the quantum mutual information (MI) of the two adjacent blocks and the von Neumann entanglement entropy (EE) (Appdenix B) at the critical point $\lambda = \lambda_c$ for q-state quantum Potts chains.

	$q = 2$	$q = 3$	$q = 4$
c	1/2	4/5	1
c (EE)	0.5007(3)	0.800(2)	1.00(4)
c (MI)	0.503(2)	0.808(4)	1.01(6)

TABLE II. Coefficients a_q and b_q fitted from the quantum mutual information (MI) of two disjoint blocks for $r = 2$ and $r = 3$ at the critical point $\lambda = \lambda_c$ for q-state quantum Potts chains with the fitting function $I_q(\ell) = a_q \log_2(\ell) + b_q$.

	$q = 2$	$q = 3$	$q = 4$
$3a_q(r = 2)$	0.317(1)	0.5103(9)	0.625(8)
$3a_q(r = 3)$	0.292(3)	0.462(4)	0.5574(3)
$b_q(r = 2)$	0.3580(7)	0.5644(4)	0.699(4)
$b_q(r = 3)$	0.276(2)	0.436(2)	0.5349(1)

dimensional infinite lattice systems shown in Fig. 1(a), the mutual information $I(\ell)$ has a universal scaling behavior such as $I(\ell) \sim \frac{c}{3} \log_2 \ell$. Actually, it is the inevitable consequence of that the reduced density matrix $\varrho_{A\cup B}$ for $S(A \cup B)$ of two adjacent blocks is the same with the reduced density matrix of lattice block of 2ℓ contiguous sites, i.e., $\varrho_{A\cup B} = \varrho_{2\ell}$, and thus $S(A \cup B) = S(2\ell)$, which implies that according to Eq. (5), the block-block mutual information of two adjacent blocks $I(\ell : \ell) = 2S(\ell) - S(2\ell) \propto \frac{c}{3} \log_2 \ell$. Furthermore, one can easily notice that $S^{\rm CC}_{A\cup B} \propto \frac{c}{3} \log_2 \ell$ for very large $\ell (\gg r)$. These facts can be interpreted that the second term of F_n in Eq. (2a) does not contribute much to the mutual information of two adjacent blocks. As a result, the mutual information of two adjacent blocks follows the universal scaling behavior of the von Neunmann entanglement entropy of single blocks in Eq. (5).

B. Mutual information of two disjoint blocks

Next, let us consider disjoint blocks for $r > 1$. The mutual information $I(\ell)$ for the disjoint blocks with $r = 2$ and $r = 3$ are plotted together in Fig. 3. As was noticed in Sec. IV B, for a given size of two blocks, the value of the block-block mutual information decreases as the lattice distance increases. In contrast to the two adjacent blocks, the reduced density matrix of two disjoint blocks with $r \neq 1$ in Fig. 1(b) is not the same with the reduced density matrix of lattice block of 2ℓ contiguous sites, i.e., $\varrho_{A\cup B} \neq \varrho_{2\ell}$ and thus $S(A \cup B) \neq S(2\ell)$. Compared to the cases of the two adjacent blocks, one may expect that the second term of F_n for the disjoint blocks in Eq. (2a) would contribute much to the block-block mutual information. Similar to the cases of the adjacent blocks for all $q = 2$, 3, and 4, the mutual information with $r = 2$ and $r = 3$ increase as the size of the lattice blocks ℓ increases. Interestingly, the mutual information for the disjoint blocks seem to exhibit the logarithmic increasing behaviors with the size of the lattice blocks ℓ. For a comparison to the cases of adjacent blocks, we perform a numerical best fit with the fitting function $I_q(\ell) = a_q \log_2 \ell + b_q$. The numerical fitting coefficients a_q and b_q are summarized in Table II. Noticeably, the values of the coefficients $3a_q$ for $r = 2$ and $r = 3$ are very different from the values of the central charges, respectively. The numerical fitting coefficients $3a_q$ show a common feature, that is, similar to the central charges, the values of the coefficients $3a_q$ seem to be distinguishable each other for different q. For the larger distance r, the coefficient $3a_q$ becomes smaller. The coefficient $a_q(r)$ has a largest value corresponding to $a_q(r = 1)$, i.e., the central charge shown in Tables I and II.

IV. SCALING BEHAVIOR OF BLOCK-BLOCK MUTUAL INFORMATION

For strongly correlated systems, characteristic scaling behaviors of conventional (two-point) spatial correlations can quantify their property. Similarly, the mutual information, as the total amount of correlations including classical and quantum correlations, can characterize strongly correlated systems. The scaling behavior of two-point (site) spatial mutual information has been studied and discussed its universality [21] in one-dimensional critical systems. Thus, in this section we study how the block-block mutual information $I(A : B)$ between the two lattice blocks with $\ell_A = \ell_B = \ell$ at the critical point changes as the lattice distance r increases. The effects of the lattice-block size on the behaviors of mutual information will be investigated. We will then consider various sizes of lattice blocks in investigating scaling behaviors of block-block mutual information. The detailed behaviors of mutual information will be discussed for quantum q-state Potts model in Sec. IV A. For the transverse-field spin-1/2 XY model, we will present a summary of scaling of mutual information in Sec. IV B and the detailed discussion in Appendix C.

A. Block-block mutual information critical exponent η^I for quantum q-state Potts model

Let us first consider the one-dimensional quantum q-state Potts model. For $q = 2$ (Ising chain), we plot the mutual information $I(r)$ as a function of the lattice distance r in the left of Fig. 4. For a given truncation dimension, the plot shows that the mutual information decreases as the lattice distance r increases. With the bigger truncation dimension, the linear region of the log-log plot gets wider and the slope of the linear region seems to be readily saturated for the truncation dimension $\chi = 150$ in the left of Fig. 4. This tendency implies that similar to the power-law behavior of the von Neumann entropy in Refs. [31,41], the mutual information undergoes a power-law decay to zero if the truncation dimension χ increases to the thermodynamic limit. Then the mutual information seems to decay linearly to zero, i.e., $I(A : B) \to 0$ as $r \to \infty$. This shows that for very large separation of the two lattice blocks, $S(A \cup B) \simeq S_A + S_B$. Such behaviors of the mutual information $I(A : B)$ reveal with the lattice distance r for all the sizes of lattice blocks, i.e., in Figs. 4(a) $\ell = 2$, 4(b) $\ell = 3$, and 4(c) $\ell = 4$.

To confirm the power-law decay of mutual information $I(r)$, we perform a numerical fit for the linear region of mutual information $I(r)$ with the fitting function, $\log_2 I(r) = -\eta^I \log_2 r + a_0$, where η^I corresponds to an exponent of power-law decay and a_0 is a fitting constant. In the right of Fig. 4, we plot the slopes $\eta^I(\chi)$ of the linear regions as a function of the truncation dimension χ with the fitting error bars [60]. The $\eta^I(\chi)$ decreases monotonically to a saturated value as the truncation dimension χ increases. To obtain the exponent η^I_∞ of mutual information in the thermodynamic limit $\chi \to \infty$, we extrapolate the exponents for various truncation dimensions in the right of Fig. 4. The extrapolation

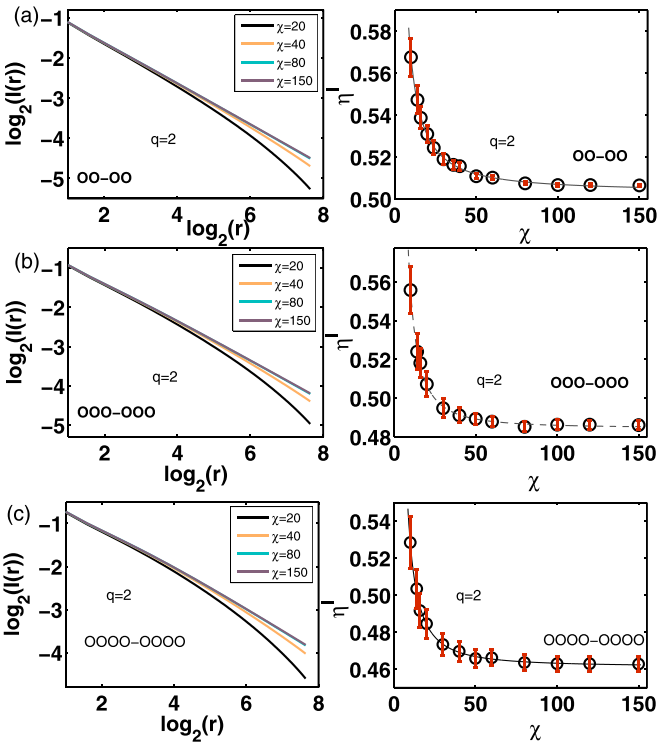

FIG. 4. Mutual information $I(r)$ as a function of the lattice distance $r = |i - j|$ for various truncation dimensions (left) and mutual information exponent $\eta^I(\chi)$ as a function of truncation dimension χ (right) with the block lengths $\ell_A = \ell_B = \ell$, i.e., (a) $\ell = 2$, (b) $\ell = 3$, and (c) $\ell = 4$ for Ising chain ($q = 2$). Mutual information exponent $\eta^I(\chi)$ (right) is extracted from the numerical fitting of the mutual information $I(\chi)$ (left) with the fitting function $\log_2 I(r) = -\eta^I \log_2 r + a_0$ for the power-law decaying part. The detailed discussions are in the text.

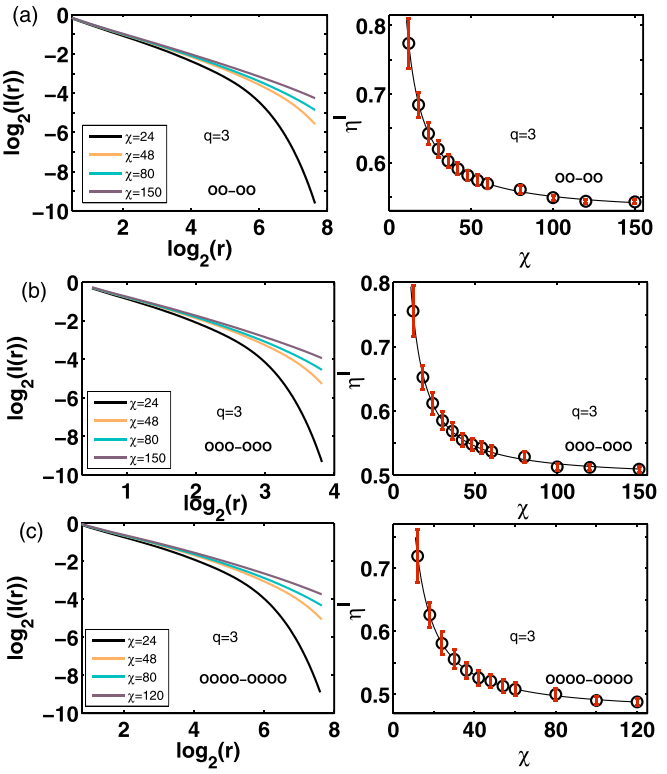

FIG. 5. Mutual information $I(r)$ as a function of the lattice distance $r = |i - j|$ for various truncation dimensions (left) and mutual information exponent $\eta^I(\chi)$ as a function of truncation dimension χ (right) with the block lengths $\ell_A = \ell_B = \ell$, i.e., (a) $\ell = 2$, (b) $\ell = 3$, and (c) $\ell = 4$ for three-state Potts chain ($q = 3$). Mutual information exponent $\eta^I(\chi)$ (right) is extracted from the numerical fitting of the mutual information $I(\chi)$ (left) with the fitting function $\log_2 I(r) = -\eta^I \log_2 r + a_0$ for the power-law decaying part. The detailed discussions are in the text.

functions are employed as a form of $\eta^I(\chi) = \eta^I_0 \chi^\alpha + \eta^I_\infty$. The numerical estimates of the critical exponent η^I_∞ of mutual information in the thermodynamic limit are given as (a) $\eta^I_0 = 1.2(2)$, $\alpha = -1.26(9)$ and $\eta^I_\infty = 0.503(1)$ for $\ell = 2$, (b) $\eta^I_0 = 3.5(9)$, $\alpha = -1.7(1)$ and $\eta^I_\infty = 0.485(1)$ for $\ell = 3$, and (c) $\eta^I_0 = 2.4(8)$, $\alpha = -1.6(1)$ and $\eta^I_\infty = 0.461(2)$ for $\ell = 4$. For the bigger size of lattice block, the critical exponent η^I_∞ becomes smaller. This means that the larger the lattice block, the slower the decaying rate of block-block information as the lattice distance r increases. In contrast to the mutual information, the von Neumann entropy was shown to be scaled as $S_{AB} \sim r^{-1/2}$ independent on the block sizes in Refs. [31,41].

For three-state Potts model ($q = 3$), in the left of Fig. 5, we display the block-block mutual information $I(r)$ as a function of the lattice distance r for various truncation dimensions χ. In Figs. 5(a)–5(c), the sizes of lattice blocks are chosen respectively as (a) $\ell = 2$, (b) $\ell = 3$, and (c) $\ell = 4$. For given truncation dimensions, the plots show that the mutual information decreases monotonically as the lattice distance r between the two lattice blocks increases. Similar to the case of $q = 2$, as the truncation dimension χ increases, the linear region of the plot becomes wider. For $\chi = 150$ in the left of Fig. 5, the log-log plot seems to be almost straight in the range of the plot. Regardless of the size of lattice block ℓ, such similar straight behaviors of mutual information $I(r)$ are noticeable. To analyze a characteristic behavior of the mutual information, we adapt the approach for $q = 2$. Using the fitting function, $\log_2 I(r) = -\eta^I \log_2 r + a_0$, we perform the numerical fit for the linear region of mutual information $I(r)$ in the right of Fig. 5. The slopes $\eta^I(\chi)$ of the linear regions are plotted as a function of the truncation dimension χ with the fitting error bars, which shows the monotonic decrement of η^I with the increment of truncation dimension χ. The extrapolation of the exponents is performed with the function, $\eta^I(\chi) = \eta^I_0 \chi^\alpha + \eta^I_\infty$. We estimate the critical exponent η^I_∞ of the mutual information in the thermodynamic limit as (a) $\eta^I_0 = 3.5(4)$, $\alpha = -1.07(5)$ and $\eta^I_\infty = 0.525(4)$ for $\ell = 2$, (b) $\eta^I_0 = 4.7(9)$, $\alpha = -1.16(8)$ and $\eta^I_\infty = 0.496(6)$ for $\ell = 3$, and (c) $\eta^I_0 = 4.7(5)$, $\alpha = -1.19(5)$ and $\eta^I_\infty = 0.472(3)$ for $\ell = 4$. For $q = 3$, the estimates of the critical exponent $\eta^I_\infty(\ell)$ show that the bigger the size of lattice block ℓ, the smaller the $\eta^I_\infty(\ell)$. Consequently, it is shown that similar to the Ising chain for $q = 2$, the mutual information $I(r)$ for $q = 3$ follows an asymptotic power-law scaling, but the scaling exponent differs from that for the Ising chain.

The critical exponents for $q = 2$ and $q = 3$ seem to be distinguishable each other for a given lattice-block size. Then let us consider the critical point of the four-state quantum Potts

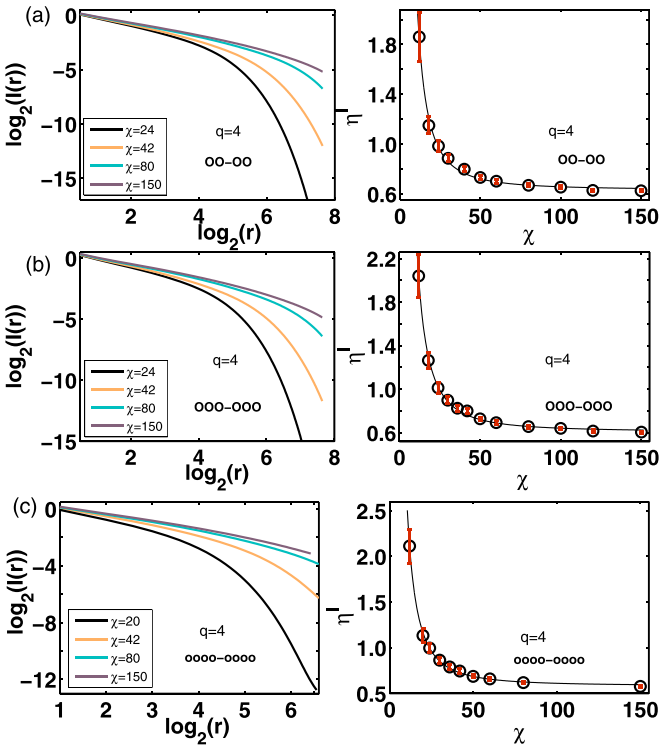

FIG. 6. Mutual information $I(r)$ as a function of the lattice distance $r = |i - j|$ for various truncation dimensions (left) and mutual information exponent $\eta^I(\chi)$ as a function of truncation dimension χ (right) with the block lengths $\ell_A = \ell_B = \ell$, i.e., (a) $\ell = 2$, (b) $\ell = 3$, and (c) $\ell = 4$ for four-state Potts chain ($q = 4$). Mutual information exponent $\eta^I(\chi)$ (right) is extracted from the numerical fitting of the mutual information $I(\chi)$ (left) with the fitting function $\log_2 I(r) = -\eta^I \log_2 r + a_0$ for the power-law decaying part. The detailed discussions are in the text.

model ($q = 4$) belonging to another universality class. We calculate the mutual information $I(r)$ for the four-state quantum Potts model ($q = 4$). Figure 6 shows the mutual information $I(r)$ as a function of the lattice-distance r for the sizes of lattice blocks (a) $\ell = 2$, (b) $\ell = 3$, and (c) $\ell = 4$. Similar to the cases of $q = 2$ and $q = 3$, the mutual information $I(r)$ for $q = 4$ exhibit a power-law decaying tendency as the truncation dimension χ increases. By using the same numerical method for $q = 2$ and $q = 3$, we estimate the critical exponents of the mutual information $I(r)$ for the block lengths $\ell = 2$, $\ell = 3$, and $\ell = 4$ in the right of Fig. 6. Performing the extrapolation with the fitting function $\eta^I(\chi) = \eta^I_0 \chi^\alpha + \eta^I_\infty$, we get the fitting results as (a) $\eta^I_0 = 115(73)$, $\alpha = -1.8(3)$ and $\eta^I_\infty = 0.63(4)$ for $\ell = 2$, (b) $\eta^I_0 = 118(43)$, $\alpha = -1.8(1)$ and $\eta^I_\infty = 0.61(3)$ for $\ell = 3$, and (c) $\eta^I_0 = 166(54)$, $\alpha = -1.9(1)$ and $\eta^I_\infty = 0.58(3)$ for $\ell = 4$. As expected from the cases of $q = 2$ and $q = 3$, the exponent η^I_∞ is smaller for $\ell = 3$ than for $\ell = 2$. Undeniably, the exponent η^I_∞ is smaller for $\ell = 4$ than for $\ell = 3$. For a given lattice-block size, then the exponent η^I_∞ has a distinguishable value from those of $q = 2$ and $q = 3$.

For comparison, we summarize our numerical estimates of critical exponents η^I_∞ at the critical points for one-dimensional quantum q-state Potts model in Table III. It

TABLE III. Critical exponents $\eta^I_\infty(q, \ell)$ of block-block mutual information $I(A : B)$ for various lattice-block sizes $\ell_A = \ell_B = \ell$ at the critical points for one-dimensional quantum q-state Potts model.

$\eta^I_\infty(q, \ell)$	$\ell = 2$	$\ell = 3$	$\ell = 4$
$q = 2$	0.503(1)	0.485(1)	0.461(2)
$q = 3$	0.525(4)	0.496(6)	0.472(3)
$q = 4$	0.63(4)	0.61(3)	0.58(3)

is shown that for all of $q = 2$, 3, and 4, the block-block mutual information $I(r)$ undergo an asymptotic power-law scaling behavior at the critical points and the critical exponents become smaller for bigger lattice blocks. These can be a characteristic feature of block-block mutual information for one-dimensional critical systems. Depending on q, i.e., the universality class, the critical exponents $\eta^I(q, \ell)$ seem to be given different values each other.

B. Block-block mutual information critical exponent η^I for transverse field spin-1/2 XY model

To clarify more about universal feature of the algebraic decay of block-block mutual information in one-dimensional critical systems, we consider the transverse-field spin-1/2 XY model [61–66] described by the Hamiltonian

$$H_{XY} = -\sum_{i=-\infty}^{\infty} \left(\gamma_+ \sigma_i^x \sigma_{i+1}^x + \gamma_- \sigma_i^y \sigma_{i+1}^y + h\, \sigma_i^z\right), \quad (7)$$

where $\sigma^{x,y,z}$ are the Pauli spin operators and $\gamma_\pm = (1 \pm \gamma)/2$. This model has two parameters, i.e., the anisotropy interaction parameter γ and the transverse magnetic field h.

As is known, the transverse-field spin-1/2 XY model has two critical lines, i.e., (i) the Ising transition lines with the central charge $c = 1/2$ for $\gamma \neq 0$ and $h = \pm 1$, and (ii) the anisotropy transition line with the central charge $c = 1$ for $\gamma = 0$ and $-1 < h < 1$.

For $\gamma = 1$, the XY model reduces to the Ising Hamiltonian for $q = 2$ in Eq. (3). Thus, in terms of the two parameters, $(\gamma, h) = (1.0, 1.0)$ corresponds to the critical point of the Ising Hamiltonian. The block-block mutual information at $(\gamma, h) = (1.0, 1.0)$ has been studied in Fig. 4 in Sec. IV A. For comparison with $(\gamma, h) = (1.0, 1.0)$, we choose $(\gamma, h) = (0.5, 1.0)$ on the Ising transition line belonging to the same university class, i.e., the Ising universality class. Also another two parameter sets $(\gamma, h) = (0.0, 0.0)$ and $(0.0, 0.5)$ are chosen on the anisotropy transition line belonging to the Gaussian university class.

For the three parameter sets, we calculate the mutual information $I(A : B)$ with the lattice blocks $\ell_A = \ell_B = \ell = 2$, 3, and 4. Similar to the one-dimensional q-state Potts model, the block-block mutual information exhibit similar power-law decaying behaviors (see the details in Appendix C). In Table IV, their critical exponents are estimated and summarized with the case of the Ising critical point ($q = 2$). Table IV shows clearly that the critical exponent $\eta^I_\infty(\gamma, h)$ decreases as the size of lattice block ℓ increases. For each given lattice block ℓ, the two critical exponents $\eta^I(\gamma, h)$ of the mutual information $I(r)$ at $(\gamma, h) = (1.0, 1.0)$ and $(0.5, 1.0)$ display

TABLE IV. Critical exponents $\eta^I_\infty(\gamma, h, \ell)$ of block-block mutual information $I(A:B)$ for various lattice-block sizes $\ell_A = \ell_B = \ell$ on the two critical lines of one-dimensional quantum transverse-field spin-1/2 XY model. For comparison, the estimates for Ising model are from Table III for $q = 2$.

$\eta^I_\infty(\gamma, h)$	$\ell = 2$	$\ell = 3$	$\ell = 4$
XY $(\gamma = 0.0, h = 0.0)$	0.999(4)	0.970(8)	0.926(5)
XY $(\gamma = 0.0, h = 0.5)$	1.008(4)	0.972(4)	0.922(6)
XY $(\gamma = 0.5, h = 1.0)$	0.501(6)	0.483(3)	0.452(6)
Ising $(q = 2)$ $(\gamma = 1.0, h = 1.0)$	0.503(1)	0.485(1)	0.461(2)

a very close value each other. The two critical exponents at $(\gamma, h) = (0.0, 0.0)$ and $(0.0, 0.5)$ also have a very close value each other. Moreover, it is shown that in accordance with the Ising universality class or the Gaussian universality class, the values of the critical exponents can be distinguishable each other for a given size of lattice block.

V. BLOCK-BLOCK CORRELATION AND THE UPPER BOUND

As usual two-point correlation functions, the block-block correlation function for the two blocks A and B can be defined as

$$C^{\alpha_A\alpha_B}(A:B) = \left\langle \mathcal{O}_A^{\alpha_A} \otimes \mathcal{O}_B^{\alpha_B} \right\rangle_g - \left\langle \mathcal{O}_A^{\alpha_A} \right\rangle_g \left\langle \mathcal{O}_B^{\alpha_B} \right\rangle_g, \tag{8}$$

where $\langle \cdots \rangle_g$ indicate the expectation values of the observables with the ground-state wave function $|\psi_g\rangle$ and the local observables for the two blocks are $\mathcal{O}_A^{\alpha_A} = \mathcal{O}_i^{\alpha_1} \otimes \mathcal{O}_{i+1}^{\alpha_{i+1}} \otimes \ldots \otimes \mathcal{O}_{\ell_A}^{\alpha_{\ell_A}}$ and $\mathcal{O}_B^{\alpha_B} = \mathcal{O}_j^{\alpha_j} \otimes \mathcal{O}_{j+1}^{\alpha_{j+1}} \otimes \ldots \otimes \mathcal{O}_{\ell_B}^{\alpha_{\ell_B}}$. Here α_is denote the local observables at site i and $\alpha_{A/B}$ indicate a set of local observables for the blocks A and B, for instance, $\alpha_A = \alpha_A(\alpha_i, \alpha_{i+1}, \ldots, \alpha_{\ell_A})$ and $\alpha_B = \alpha_B(\alpha_i, \alpha_{i+1}, \ldots, \alpha_{\ell_B})$. In terms of the reduced density matrices, the block-block correlation can be written with $\mathcal{O}^{\alpha_A\alpha_B} \equiv \mathcal{O}_A^{\alpha_A} \otimes \mathcal{O}_B^{\alpha_B}$ as

$$C^{\alpha_A\alpha_B}(A:B) = \mathrm{Tr}[\mathcal{O}^{\alpha_A\alpha_B}\rho(A:B)], \tag{9a}$$

$$\rho(A:B) = \rho_{A\cup B} - \rho_A \otimes \rho_B, \tag{9b}$$

where $\rho(A:B)$ can be called correlation density matrix [67,68] and $\rho(A:B) = 0 (\rho_{A\cup B} = \rho_A \otimes \rho_B)$ if there is no correlation between the two blocks A and B. If the local Hilbert space per site is q, then the $\rho(A:B)$ can be represented as a $q^{\ell_A+\ell_B} \times q^{\ell_A+\ell_B}$ matrix with $q^{2(\ell_A+\ell_B)}$ elements with the sizes of the the blocks ℓ_A and ℓ_B.

For block-block correlation functions, the number of sets of the local observables for the block A and B is determined with the possible combinations of the local observables, i.e., $m^{\ell_A+\ell_B}$, where m is the number of local observable at each site i. As the sizes of the blocks A and B increase, the number of block-block correlation functions increases significantly. It could be a highly nontrivial challenge to extract useful information from calculating directly the number of block-block correlation functions. Recently, it was shown in Ref. [68] that the Schatten one-norm of the correlation density matrix $\rho(A:B)$ yields an upper bound for the block-block correlations as follows:

$$|C^{\alpha_A\alpha_B}| \leqslant \|\rho(A:B)\|_1 = \sum_{\mu=1}^{q^{\ell_A+\ell_B}} |p_{AB}^\mu|, \tag{10}$$

where p_{AB}^μ are the eigenvalues of $\rho(A:B)$. This upper bound of block-block correlations can give a common feature of block-block correlations. Thus, in our study, we consider the upper bound of block-block correlations C in Eq. (10) for the truncation dimension $\chi = 150$.

Using the iMPS ground-state wave function for $\chi = 150$, we calculate the upper bound of block-block correlations at the critical points of the quantum q-state model and at the chosen critical points of the quantum transverse field spin-1/2 XY model. We plot the upper bound C as a function of the lattice distance $r = |i - j|$ in Fig. 7 for the quantum q-state model and in Fig. 8 for the quantum transverse field spin-1/2 XY model. We can notice that similar to the linear regions of the mutual information $I(r)$ for $\chi = 150$, all of the upper bounds of block-block correlations decay to zero and have linear regions. To estimate the exponents of the power-law decaying parts, we perform the numerical fitting with the fitting function $\log_2(C) = -\eta \log_2 |i - j| + a_0$. The critical exponents for $\chi = 150$ are displayed in Tables V and VI for the quantum q-state model and the quantum transverse field spin-1/2 XY model, respectively. Similar to the mutual information, as the size of lattice block ℓ becomes bigger, the $\eta_{\chi=150}(\ell)$ becomes smaller. For the quantum q-state Potts model, the critical exponents $\eta_{\chi=150}(q, \ell)$ seem to be different each other, depending on q, i.e., the universality class in Table V. However, compared to the exponents of the mutual information, the difference between the exponents seems not to be very big for a given size of the block. For the transverse-field spin-1/2 XY model, according to the Ising

TABLE V. Critical exponents $\eta_{\chi=150}(q, \ell)$ of the upper bound of block-block correlation $C(A:B)$ for various lattice-block sizes $\ell_A = \ell_B = \ell$ at the critical points $\lambda_c = 1$ for one-dimensional quantum q-state Potts model. The truncation dimension is $\chi = 150$.

$\eta_{\chi=150}(q, \ell)$	$\ell = 2$	$\ell = 3$	$\ell = 4$
$q = 2$	0.238(1)	0.224(2)	0.212(2)
$q = 3$	0.269(2)	0.247(3)	0.240(3)
$q = 4$	0.299(4)	0.289(6)	—

TABLE VI. Critical exponents $\eta_{\chi=150}(\gamma, h, \ell)$ of the upper bound of block-block correlation $C(A:B)$ for various lattice-block sizes $\ell_A = \ell_B = \ell$ on the two critical lines of one-dimensional quantum transverse-field spin-1/2 XY model. The truncation dimension is $\chi = 150$. For comparison, the estimates for Ising model are from Table IV for $q = 2$.

$\eta_{\chi=150}(\gamma, h, \ell)$	$\ell = 2$	$\ell = 3$	$\ell = 4$
XY $(\gamma = 0.0, h = 0.0)$	0.519(7)	0.48(1)	0.45(1)
XY $(\gamma = 0.0, h = 0.5)$	0.521(5)	0.491(8)	0.45(1)
XY $(\gamma = 0.5, h = 1.0)$	0.238(2)	0.229(2)	0.219(3)
Ising $(q = 2)$ $(\gamma = 1.0, h = 1.0)$	0.238(1)	0.224(2)	0.212(2)

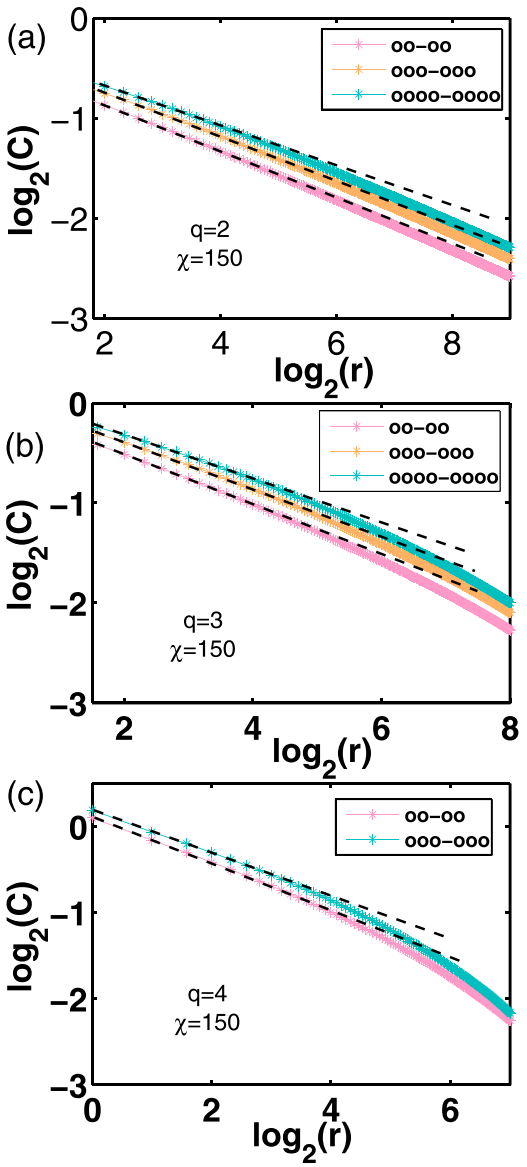

FIG. 7. Block-block correlation as a function of the lattice distance $r = |i - j|$ for quantum q-state Potts model for various block sizes $\ell_A = \ell_B = \ell$ with the truncation dimension $\chi = 150$ at the critical point $\lambda_c = 1$. We consider the block sizes $\ell = 2$, 3, and 4 for (a) $q = 2$ and (b) $q = 3$. For (c) $q = 4$, the block sizes $\ell = 2$ and 3 are considered.

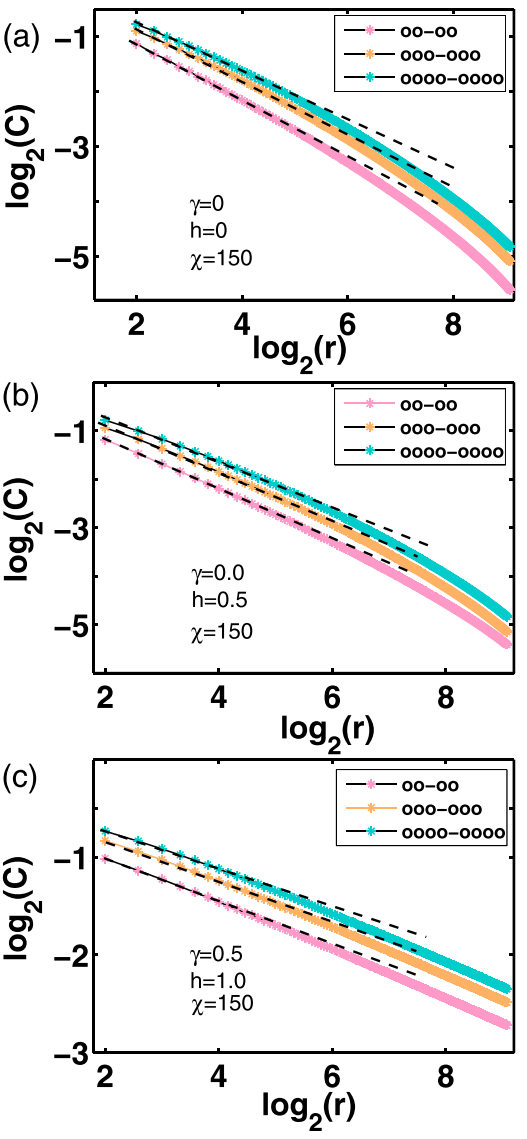

FIG. 8. Block-block correlation as a function of the lattice distance $r = |i - j|$ for quantum XY model for various block sizes $\ell_A = \ell_B = \ell$ with the truncation dimension $\chi = 150$ at points (a) $(\gamma, h) = (0.0, 0.0)$, (b) $(\gamma, h) = (0.0, 0.5)$, and (c) $(\gamma, h) = (0.5, 1.0)$, respectively. The block lengths $\ell = 2$, 3, and 4 are considered.

universality class or the Gaussian universality class, the values of the critical exponents $\eta_{\chi=150}(\gamma, h)$ seem to be distinguishable each other for a given size of lattice block in Table VI. Consequently, we find that the upper bounds of block-block correlations show a very similar tendency to the block-block mutual information. The exponents of their linear regions depend on the lattice-block size. The bigger the lattice block, the smaller the critical exponent.

The block-size dependence of the exponents follows the block-size dependence of the exponents of the mutual information. To compare with the exponents of the mutual information in Sec. IV, we list the estimate critical exponents of the mutual information for the truncation dimension $\chi = 150$ in Table VII. The ratios $K = \eta^I_{\chi=150}/\eta_{\chi=150}$ are also listed in Table VII. Table VII shows that the ratios K have values quite close to 2. It seems that regardless of the universality classes and the size of the blocks, the critical exponents of the mutual information have about twice the value of the critical exponents of the upper bound of the block-block correlations, i.e., $\eta^I_{\chi=150}/\eta_{\chi=150} \sim 2$.

VI. SUMMARY

The block-block mutual information defined by the von Neumann entropies has been numerically investigated in the one-dimensional q-state quantum Potts model and the transverse-field spin-1/2 XY model. To calculate the reduced density matrices for the mutual information, the ground-state wave function of the infinite-size lattice chain is obtained by using the iTEBD algorithm in the iMPS representation. We

TABLE VII. Critical exponents $\eta^I_{\chi=150}$ of the block-block mutual information $I(A:B)$ and the ratio $K=\eta^I_{\chi=150}/\eta_{\chi=150}$ for various lattice-block sizes $\ell_A=\ell_B=\ell$ for the quantum q-state Potts model and the quantum transverse-field spin-1/2 XY model.

$\eta^I_{\chi=150}$	$\ell=2$	$\ell=3$	$\ell=4$
XY ($\gamma=0.0, h=0.0$)	1.029(8)	1.00(1)	0.96(1)
XY ($\gamma=0.0, h=0.5$)	1.041(7)	0.996(9)	0.95(1)
XY ($\gamma=0.5, h=1.0$)	0.5109(7)	0.488(3)	0.460(4)
Ising or $q=2$ ($\gamma=1.0, h=1.0$)	0.5065(6)	0.486(2)	0.463(4)
$q=3$	0.543(3)	0.509(5)	0.488(6)
$q=4$	0.626(8)	0.606(9)	0.58(1)
$K=\eta^I_{\chi=150}/\eta_{\chi=150}$	$\ell=2$	$\ell=3$	$\ell=4$
XY ($\gamma=0.0, h=0.0$)	1.98(4)	2.08(7)	2.11(9)
XY ($\gamma=0.0, h=0.5$)	2.00(3)	2.03(5)	2.10(9)
XY ($\gamma=0.5, h=1.0$)	2.13(2)	2.13(3)	2.10(5)
Ising or $q=2$ ($\gamma=1.0, h=1.0$)	2.12(1)	2.17(3)	2.18(4)
$q=3$	2.02(3)	2.06(5)	2.03(5)
$q=4$	2.09(5)	2.10(7)	—

first considered the block-block mutual information $I_q(A:B)$ between the two blocks for $\ell_A=\ell_B=\ell$. For the spontaneous symmetry breaking in one-dimensional q-state quantum Potts model, we found that all q degenerate ground states give the same block-block mutual information. As the transverse-field λ varies, for both the two adjacent and disjoint blocks, the block-block mutual information $I_q(\ell)$ exhibit a singular behavior at the critical point, which indicates that the quantum phase transition occurs at the singular point and thus can be detected by using the block-block mutual information. For a given lattice distance, the critical mutual information $I_q(\ell)$ seems to show a logarithmic leading behavior, i.e., $I_q(\ell)\sim a_q\log_2\ell+b_q$ for both the two adjacent and disjoint blocks. For the case of two adjacent blocks ($r=1$), the numerical coefficients of the logarithm term are shown to be a close value of the central charge c_q in Table I in our iMPS approach, as they should be. While for the two disjoint blocks with $r=2$ and $r=3$, the coefficients of the logarithmic terms, not giving a close value of the central charges, depend on the lattice distance r, as shown in Table II.

Next, we have studied the block-block mutual information with respect to the lattice distance. In both the ordered and the disordered phases, as the distance r between two lattice blocks increases, the block-block mutual information exponentially decay to zero. For each q, the mutual information correlation length ξ_M is dependent of the lattice-block size, i.e., the larger the size of the lattice blocks, the longer the correlation length ξ_M. For the ordered and the disordered phases, the detailed discussion on the block-block mutual information is given in Appendix D. Whereas, regardless of the size of lattice block ℓ, the mutual information $I(\ell)$ seems to undergo a power-law decay at the critical points.

By using the extrapolation of the exponents of $I(\ell)$ for finite truncation dimensions, the critical exponents η^I_∞ were estimated in the thermodynamic limit. To see clearly the change of critical exponent for various sizes of lattice blocks ℓ, we plot the critical exponent η^I_∞ as a function of ℓ in Fig. 9 based on Table III for the q-state quantum Potts model and Table IV for the transverse-field spin-1/2 XY model. It

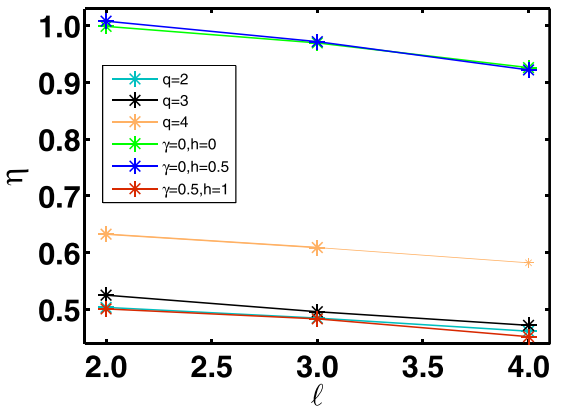

FIG. 9. Block-block mutual information exponent $\eta^I_\infty(\ell)$ as a function of the lattice-block size ℓ for one-dimensional q-state quantum Potts model in Table III and the transverse-field spin-1/2 XY model in Table IV.

is shown clearly that the larger the lattice-block size ℓ, the smaller the critical exponent η^I_∞. The decreasing tendencies of the mutual information $I(\ell)$ are similar each other in all cases as the size of lattice block ℓ increases. For a given lattice-block size ℓ, the critical exponents of $I(\ell)$ for the same universality class seem to have very close values each other in Table IV in Sec. IV B. Whereas for different universality classes, the values of critical exponents are different distinguishably.

We have also investigated the upper bound of block-block correlations that is given as the Shatten-one norm of the correlation density matrix. The Shatten-one norm show a power-law decay to zero at the critical systems for the both quantum q-state Potts model and transverse-field spin-1/2 XY model. Similar to the critical exponents of the mutual information, the larger the lattice-block size ℓ, the smaller the critical exponent $\eta_{\chi=150}$. The exponents of the upper bounds with the truncation dimension $\chi=150$ for the same universality class seem to have very close values each other, as shown in Tables V and VI. Regardless of the universality classes and the size of the blocks, the critical exponent of the mutual information was shown to have an interesting relation with the exponent of Shatten-one norm for the upper bound of the block-block correlation, i.e., $\eta^I_{\chi=150}\sim 2\eta_{\chi=150}$.

ACKNOWLEDGMENTS

Y.-W.D. is supported in part by the National Natural Science Foundation of China (Grant No. 11805285), and the Fundamental Research Funds for the Central Universities (Grant No. 2019CDXYXDWL30030). X.-H.C. is supported by Talent Introduction Research Funds of CQWU (Grant No. R2019FXCo7). S.Y.C. acknowledges support in part from the National Natural Science Foundation of China (Grants No. 11674042 and No. 11174375).

APPENDIX A: MUTUAL INFORMATION WITH TWO ADJACENT BLOCKS

In Sec. IV B we discussed the characteristic behaviors of the block-block mutual information for the two disjoint blocks, shown in Fig. 1(b), as a function of the transverse-field

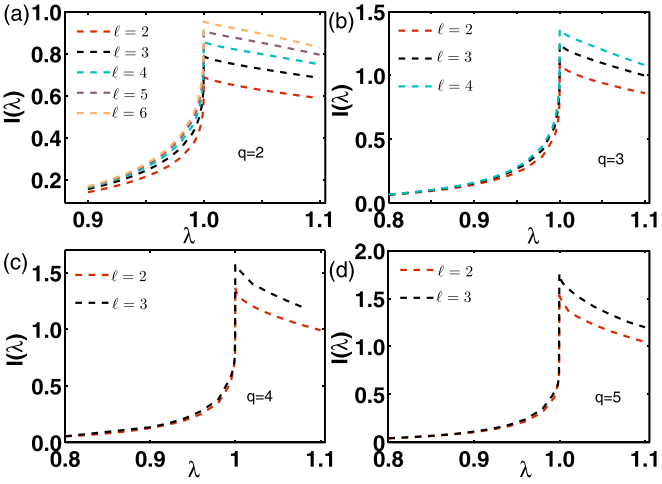

FIG. 10. Mutual information $I_q(\lambda)$ of two adjacent lattice blocks with (a) $q = 2$, (b) $q = 3$, (c) $q = 4$, and (d) $q = 5$ as a function of the transverse field λ for one-dimensional q-state quantum Potts model with various sizes of lattice blocks ℓ.

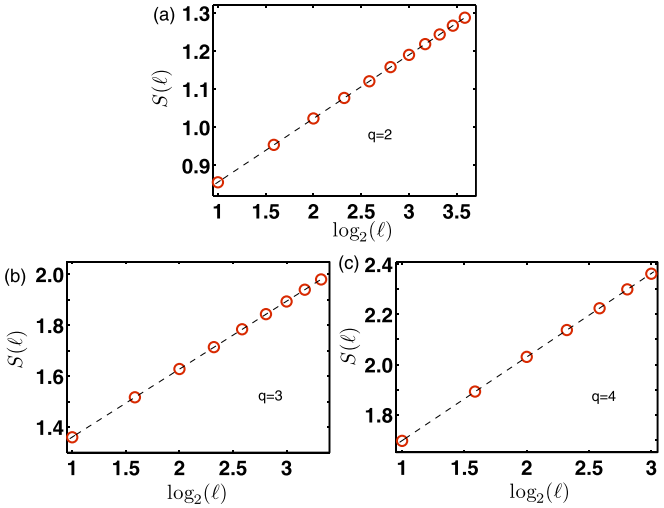

FIG. 11. Von Neumann entropy $S(\ell)$ as a function of the block length ℓ at the critical point $\lambda = \lambda_c$ for quantum Potts chains with (a) $q = 2$, (b) $q = 3$, and (c) $q = 4$. The lines are the numerical fitting functions $S_q(\ell) = f_q \log_2 \ell + g_q$ with the numerical coefficients f_q and g_q. The detailed discussions are in the text.

λ. In this Appendix, for comparison, we present the mutual information for the two adjacent blocks shown in Fig. 1(a). We plot the mutual information as a function of the transverse field λ in Fig. 10. As the size of lattice blocks ℓ increases, the value of the block-block mutual information increases for all q. At the critical points $\lambda = 1$, one can notice the predominant singular behaviors of the mutual information. With the discussion in Sec. IV B, this implies that quantum phase transition can be captured by using block-block mutual information for both cases of two adjacent and disjoint blocks.

APPENDIX B: CENTRAL CHARGES AND BLOCK ENTANGLEMENT ENTROPY

In this Appendix, to demonstrate the reliability of our iMPS approach, we estimate the central charges from our iMPS ground states. To do this, we calculate the von Neumann entropy for various lattice block of ℓ contiguous sites in our iMPS ground states. In Fig. 11, we plot the block entanglement entropy as a function of the lattice-block size ℓ for the one-dimensional (a) $q = 2$, (b) $q = 3$, and (c) $q = 4$ state Potts models. As were predicted in Eq. (5), the entanglement entropies in Fig. 11 exhibit a logarithmic scaling behavior. This fact can be manifested by performing the numerical fits to extract the central charges with the fitting function $S_q(\ell) = f_q \log_2 \ell + g_q$. The numerical fitting coefficients f_q and g_q are given as (a) $f_2 = 0.1669(1)$ and $g_2 = 0.6892(4)$ for $q = 2$, (b) $f_3 = 0.266(8)$ and $g_3 = 1.094(2)$ for $q = 3$, and (c) $f_4 = 0.3334(13)$ and $g_4 = 1.363(3)$ for $q = 4$. From the fitting coefficients, the central charges can be estimated as $3f_q = c_q$, i.e., (a) $3f_2 = 0.5007(3)$ for $q = 2$, (b) $3f_3 = 0.800(2)$ for $q = 3$, and (c) $3f_4 = 1.00(4)$ for $q = 4$. Our estimates of the central charges c_q obtained from the von Neumann entropy $S_q(\ell)$ are in excellent agreement with the exact values as was shown in Table I. This shows that the iMPS approach gives a reliable numerical result for the central charges.

APPENDIX C: BLOCK-BLOCK MUTUAL INFORMATION FOR TRANSVERSE FIELD SPIN-1/2 *XY* MODEL

In this Appendix, we present the criticality of block-block mutual information $I(A:B)$ for the transverse field spin-1/2 XY model in Eq. (7). In the γ-h parameter space of the Hamiltonian, the four parameters are chosen on the two critical lines such as (i) $(\gamma, h) = (1.0, 1.0)$ and $(0.5, 1.0)$ on the Ising transition line and (ii) $(\gamma, h) = (0.0, 0.0)$ and $(0.0, 0.5)$ on the anisotropy transition line. In the case of the parameters $(\gamma, h) = (1.0, 1.0)$ corresponding to the Ising model ($q = 2$) in Eq. (3), the critical exponents of mutual information have been displayed in Fig. 4. The numerical results for the other parameters will then be presented in this Appendix.

Given the size of the blocks for $(\gamma, h) = (0.5, 1.0)$ on the Ising transition line, Fig. 12 displays the mutual information as a function of the lattice distance r and the numerically fitted exponents of the linear regions as a function of the truncation dimension χ. Overall behaviors of the mutual information in the left of Fig. 12 for $(\gamma, h) = (0.5, 1.0)$ can be noticed to be similar with those in the left of Fig. 4 for $(\gamma, h) = (1.0, 1.0)$, i.e., the block-block mutual information $I(r)$ decays to zero algebraically as the distance r between the two blocks increases. In the right of Fig. 12, we plot the exponents $\eta(\chi)$ of the block-block mutual information as a function of the truncation dimension χ for various sizes of lattice blocks ℓ. To get the critical exponents η_∞ in the thermodynamic limit, the extrapolations are performed with the fitting function, $\eta^I(\chi) = \eta_0^I \chi^\alpha + \eta_\infty^I$ as follows: (a) $\eta_0^I = 0.21(6)$, $\alpha = -0.6(2)$ and $\eta_\infty^I = 0.501(6)$ for $\ell = 2$, (b) $\eta_0^I = 0.4(1)$, $\alpha = -1.0(2)$ and $\eta_\infty^I = 0.483(3)$ for $\ell = 3$, and (c) $\eta_0^I = 0.4(2)$, $\alpha = -0.8(2)$ and $\eta_\infty^I = 0.452(6)$ for $\ell = 4$. One can notice that the critical exponents η_∞^I for $(\gamma, h) = (0.5, 1.0)$ are very close values for $(\gamma, h) = (1.0, 1.0)$ in Fig. 4. Note that the two parameters are in the same universality class, i.e., the Ising universality class with $c = 1/2$.

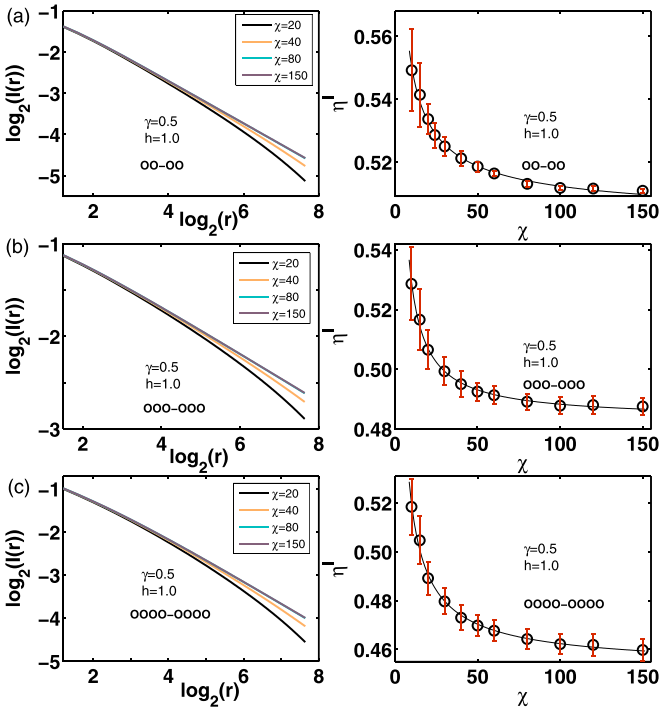

FIG. 12. Mutual information $I(r)$ as a function of the lattice distance $r = |i - j|$ for various truncation dimensions (left) and mutual information exponent $\eta^I(\chi)$ as a function of truncation dimension χ (right) with the block lengths $\ell_A = \ell_B = \ell$, i.e., (a) $\ell = 2$, (b) $\ell = 3$, and (c) $\ell = 4$ for the transverse-field spin-1/2 XY model with $(\gamma, h) = (0.5, 1.0)$. Mutual information exponent $\eta^I(\chi)$ (right) is extracted from the numerical fitting of the mutual information $I(\chi)$ (left) with the fitting function $\log_2 I(r) = -\eta^I \log_2 r + a_0$ for the power-law decaying part.

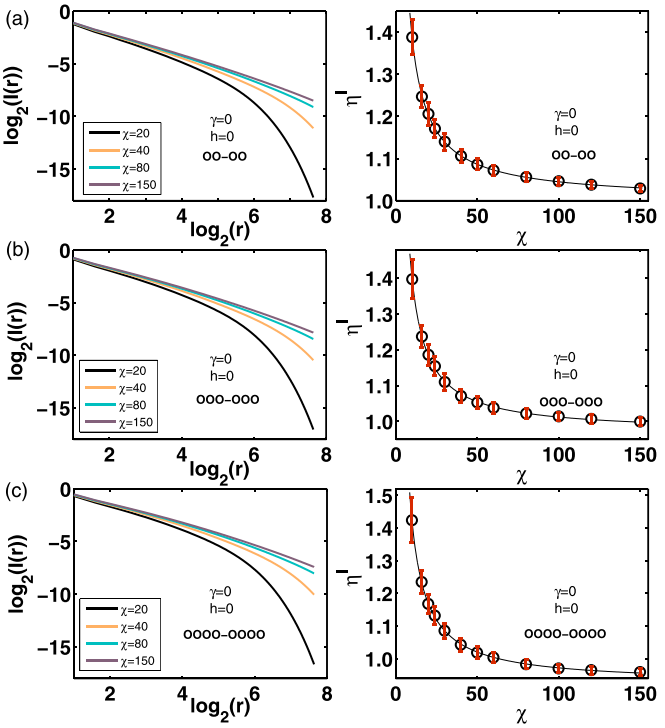

FIG. 13. Mutual information $I(r)$ as a function of the lattice distance $r = |i - j|$ for various truncation dimensions (left) and mutual information exponent $\eta^I(\chi)$ as a function of truncation dimension χ (right) with the block lengths $\ell_A = \ell_B = \ell$, i.e., (a) $\ell = 2$, (b) $\ell = 3$, and (c) $\ell = 4$ for the transverse-field spin-1/2 XY model with $(\gamma, h) = (0.0, 0.0)$. Mutual information exponent $\eta^I(\chi)$ (right) is extracted from the numerical fitting of the mutual information $I(\chi)$ (left) with the fitting function $\log_2 I(r) = -\eta^I \log_2 r + a_0$ for the power-law decaying part.

Next, we calculate the block-block mutual information for the other two parameters $(\gamma, h) = (0.0, 0.0)$ and $(\gamma, h) = (0.0, 0.5)$ on the anisotropy transition line belonging to the Gaussian universality class with $c = 1$. In Figs. 13 and 14, the block-block mutual information and their exponents are displayed for $(\gamma, h) = (0.0, 0.0)$ and $(\gamma, h) = (0.0, 0.5)$, respectively. For the sizes of lattice blocks (a) $\ell = 2$, (b) $\ell = 3$, and (c) $\ell = 4$, as the distance between two blocks increases, a noticeable common behavior is an algebraic decay of the block-block mutual information $I(r)$ to zero. For given truncation dimensions χ, we plot the exponents $\eta^I(\chi)$ of the mutual information from the fitting function $\log_2[I(r)] = -\eta^I \log_2(r) + a_0$. As shown in the right of Figs. 13 and 14, the extrapolations are performed for the critical exponents η_∞ with the function $\eta^I(\chi) = \eta_0^I \chi^\alpha + \eta_\infty^I$. For $(\gamma, h) = (0.0, 0.0)$, the numerical constants in Fig. 13 are given as (a) $\eta_0^I = 3.3(2)$, $\alpha = -0.93(3)$ and $\eta_\infty^I = 0.999(4)$ for $\ell = 2$, (b) $\eta_0^I = 4.3(5)$, $\alpha = -1.00(5)$ and $\eta_\infty^I = 0.970(8)$ for $\ell = 3$, and (c) $\eta_0^I = 5.4(4)$, $\alpha = -1.03(3)$ and $\eta_\infty^I = 0.926(5)$ for $\ell = 4$. For $(\gamma, h) = (0.0, 0.5)$, the fitting constants in Fig. 14 are determined as (a) $\eta_0^I = 3.3(2)$, $\alpha = -0.92(3)$ and $\eta_\infty^I = 1.008(4)$ for $\ell = 2$, (b) $\eta_0^I = 4.7(3)$, $\alpha = -1.06(3)$ and $\eta_\infty^I = 0.972(4)$ for $\ell = 3$, and (c) $\eta_0^I = 4.4(3)$, $\alpha = -0.99(4)$ and $\eta_\infty^I = 0.922(6)$ for $\ell = 4$. These estimates show that for a given size of lattice block ℓ, the critical exponents for $(\gamma, h) = (0.0, 0.0)$ and $(\gamma, h) = (0.0, 0.5)$ are very close values each other. However, it should be noted that the estimate values for $(\gamma, h) = (1.0, 1.0)$ and $(\gamma, h) = (0.5, 1.0)$ belonging to the Ising universality class are noticeably different from those for $(\gamma, h) = (0.0, 0.0)$ and $(\gamma, h) = (0.0, 0.5)$ belonging to the Gaussian universality class.

APPENDIX D: BLOCK-BLOCK MUTUAL INFORMATION IN THE ORDERED AND DISORDERED PHASES FOR THE QUANTUM q-STATE POTTS MODEL

In Sec. IV B, it has shown that the block-block mutual information can detect the phase transition field strength $\lambda_c = 1$ for the one-dimensional q-state quantum Potts model. For the field strength $\lambda < 1 (\lambda > 1)$, as is well-known, the one-dimensional q-state Potts model is in the ordered (disordered) phase. In the main text, we have discussed about the critical behaviors of the block-block mutual information at the critical point. In this Appendix, we will discuss the behaviors of block-block mutual information in the ordered and disordered phases.

To do this, we choose the two field strengths $\lambda = 0.9$ in the ordered phase and $\lambda = 1.1$ in the disordered phase. We calculate the block-block mutual information $I(r)$ from the ground-state wave functions with the truncation dimension

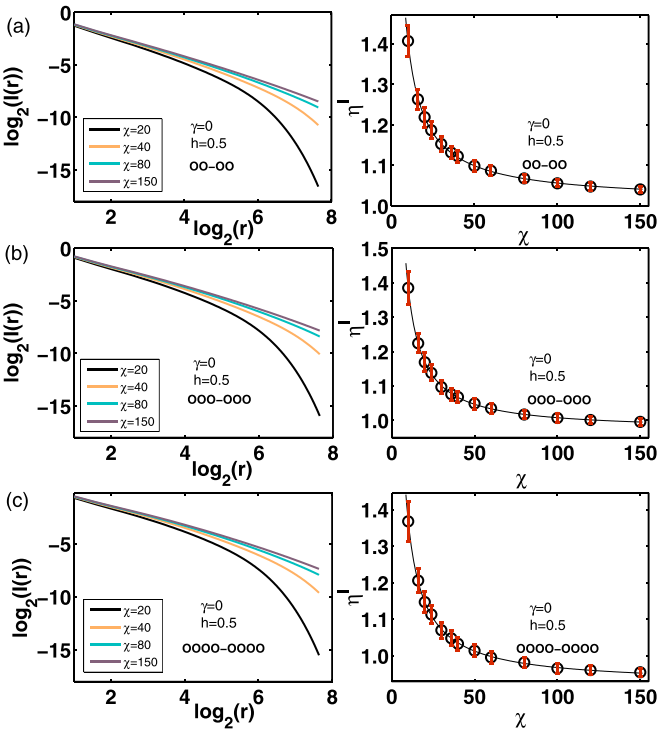

FIG. 14. Mutual information $I(r)$ as a function of the lattice distance $r = |i - j|$ for various truncation dimensions (left) and mutual information exponent $\eta^I(\chi)$ as a function of truncation dimension χ (right) with the block lengths $\ell_A = \ell_B = \ell$, i.e., (a) $\ell = 2$, (b) $\ell = 3$, and (c) $\ell = 4$ for the transverse-field spin-1/2 XY model with $(\gamma, h) = (0.0, 0.5)$. Mutual information exponent $\eta^I(\chi)$ (right) is extracted from the numerical fitting of the mutual information $I(\chi)$ (left) with the fitting function $\log_2 I(r) = -\eta^I \log_2 r + a_0$ for the power-law decaying part.

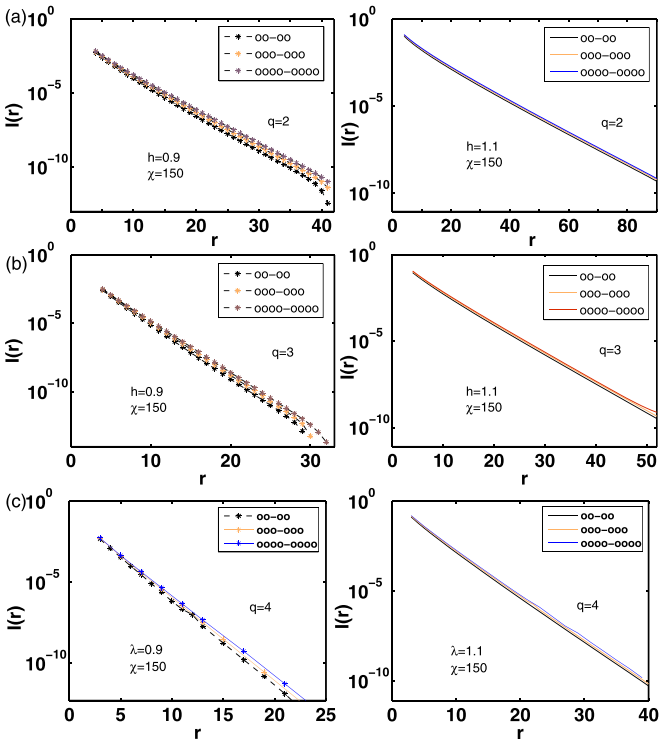

FIG. 15. Mutual information $I(r)$ for the two disjoint blocks $\ell_A = \ell_B = \ell = 2$, 3, and 4 as a function of the lattice distance $r = |i - j|$ at the field strengths $\lambda = 0.9$ (left) and $\lambda = 1.1$ (right) with truncation dimension $\chi = 150$. The exponential decaying of the block-block mutual information can be characterized by defining the decaying length ξ_M. The block-block mutual information correlation length ξ_M is extracted from the numerical fitting of the mutual information $I(r)$ with the fitting function $I(r) = c_0 e^{-r/\xi_M}$.

$\chi = 150$ for $\lambda = 0.9$ and $\lambda = 1.1$. In Fig. 15, we plot the block-block mutual information $I(r)$ as a function of the lattice distance $r = |i - j|$ for (a) $q = 2$, (b) $q = 3$, and (c) $q = 4$. For the two disjoint blocks, the three sizes of the blocks are chosen such as $\ell_A = \ell_B = \ell = 2$, 3, and 4. It can be easily noticed that for the chosen system parameter, the block-block mutual information decays exponentially with the distance. For other truncation dimensions, we have observed similar exponential-decaying behaviors of block-block mutual information.

Such exponential-decaying behaviors of the block-block mutual information in the ordered and disordered phases can be quantified by defining a characteristic decaying length, i.e., so-called mutual information correlation length ξ_M. Thus, we perform the numerical fitting to extract the mutual information correlation length ξ_M. The fitting function $I(r) = c_0 e^{-r/\xi_M}$ is employed with the numerical fitting coefficients c_0 and ξ_M. For $\lambda = 0.9$ in the order phase and $\lambda = 1.1$ in the disordered phase, the fitting results give the c_0s and ξ_Ms listed in Table VIII. In the order phase of the field strength $\lambda = 0.9$, it is shown that as the size of the two disjoint blocks ℓ increases, the mutual information correlation length ξ_M seems to increase for each q. For a given size of the disjoint blocks ℓ, the bigger q-state Potts system has the shorter ξ_M. Similar to the order phase at the field strength $\lambda = 0.9$, the disordered phase at the field strength $\lambda = 1.1$ shows that regardless of q, the block-block mutual correlation length ξ_M increases as the size of the disjoint blocks increases, and also, for a given size of the disjoint blocks ℓ, the bigger q-state Potts system has the shorter ξ_M. We have observed that for other parameters in the ordered or disordered phases, the behaviors of the block-block mutual information are shown to be very similar to those of the block-block mutual information for the chosen parameters.

TABLE VIII. Mutual information correlation length ξ_M at the field strengths $\lambda = 0.9$ and $\lambda = 1.1$ for quantum q-state Potts model with truncation dimension $\chi = 150$.

$\xi_M(q, \ell)$ at $\lambda = 0.9$	$\ell = 2$	$\ell = 3$	$\ell = 4$
$q = 2$	1.69(4)	1.77(4)	1.84(4)
$q = 3$	1.07(1)	1.118(5)	1.155(3)
$q = 4$	0.82(2)	0.87(3)	0.89(3)
$\xi_M(q, \ell)$ at $\lambda = 1.1$	$\ell = 2$	$\ell = 3$	$\ell = 4$
$q = 2$	3.64(6)	3.68(6)	3.72(6)
$q = 3$	2.24(2)	2.26(2)	2.29(2)
$q = 4$	1.617(7)	1.636(7)	1.661(6)

[1] S. Sachdev, *Quantum Phase Transitions* (Cambridge University Press, Cambridge, UK, 1999).

[2] P. M. Chaikin and T. C. Lubensky, *Pinciples of Condensed Matter Physics* (Cambridge University Press, Cambridge, UK, 1995).

[3] L. Amico, R. Fazio, A. Osterloh, and V. Vedral, Rev. Mod. Phys. **80**, 517 (2008); K. Modi, A. Brodutch, H. Cable, T. Paterek, and V. Vedral, *ibid.* **84**, 1655 (2012).

[4] R. Dorner and V. Vedral, Int. J. Mod. Phys. B **27**, 1345017 (2013).

[5] C. Adami and N. J. Cerf, Phys. Rev. A **56**, 3470 (1997).

[6] B. Groisman, S. Popescu, and A. Winter, Phys. Rev. A **72**, 032317 (2005).

[7] B. Schumacher and M. D. Westmoreland, Phys. Rev. A **74**, 042305 (2006).

[8] V. Eisler and Z. Zimborás, Phys. Rev. A **89**, 032321 (2014).

[9] A. Anfossi, P. Giorda, A. Montorsi, and F. Traversa, Phys. Rev. Lett. **95**, 056402 (2005).

[10] M. M. Wolf, F. Verstraete, M. B. Hastings, and J. I. Cirac, Phys. Rev. Lett. **100**, 070502 (2008).

[11] R. G. Melko, A. B. Kallin, and M. B. Hastings, Phys. Rev. B **82**, 100409(R) (2010).

[12] Y.-X. Chen and S.-W. Li, Phys. Rev. A **81**, 032120 (2010).

[13] R. R. P. Singh, M. B. Hastings, A. B. Kallin, and R. G. Melko, Phys. Rev. Lett. **106**, 135701 (2011).

[14] J. Um, H. Park, and H. Hinrichsen, J. Stat. Mech. (2012) P10026.

[15] J. Wilms, J. Vidal, F. Verstraete, and S. Dusuel, J. Stat. Mech. (2012) P01023.

[16] Y. Huang and J. E. Moore, Phys. Rev. B **90**, 220202(R) (2014).

[17] F. C. Alcaraz and M. A. Rajabpour, Phys. Rev. Lett. **111**, 017201 (2013).

[18] J. M. Stéphan, J. Stat. Mech. (2014) P05010; Phys. Rev. B **90**, 045424 (2014).

[19] F. C. Alcaraz and M. A. Rajabpour, Phys. Rev. B **90**, 075132 (2014).

[20] F. C. Alcaraz and M. A. Rajabpour, Phys. Rev. B **91**, 155122 (2015).

[21] Y.-W. Dai, X.-H. Chen, S. Y. Cho, H.-Q. Zhou, and D.-X. Yao, arXiv:1805.03464.

[22] H. Casini and M. Huerta, Phys. Lett. B **600**, 142 (2004).

[23] M. Caraglio and F. Gliozzi, J. High Energy Phys. 11 (2008) 076.

[24] S. Furukawa, V. Pasquier, and J. Shiraishi, Phys. Rev. Lett. **102**, 170602 (2009).

[25] P. Calabrese and J. Cardy, J. Stat. Mech. (2004) P06002.

[26] P. Calabrese, J. Cardy, and E. Tonni, J. Stat. Mech. (2009) P11001.

[27] S. Marcovitch, A. Retzker, M. B. Plenio, and B. Reznik, Phys. Rev. A **80**, 012325 (2009).

[28] H. Wichterich, J. Molina-Vilaplana, and S. Bose, Phys. Rev. A **80**, 010304(R) (2009).

[29] H. Wichterich, J. Vidal, and S. Bose, Phys. Rev. A **81**, 032311 (2010).

[30] H. Casini and M. Huerta, J. High Energy Phys. 03 (2009) 048.

[31] V. Alba, L. Tagliacozzo, and P. Calabrese, Phys. Rev. B **81**, 060411(R) (2010).

[32] M. Fagotti and P. Calabrese, J. Stat. Mech. (2010) P04016.

[33] P. Calabrese, J. Cardy, and E. Tonni, J. Stat. Mech. (2011) P01021.

[34] R. A. Santos, V. Korepin, and S. Bose, Phys. Rev. A **84**, 062307 (2011).

[35] P. Calabrese, J. Cardy, and E. Tonni, Phys. Rev. Lett. **109**, 130502 (2012).

[36] M. Fagotti, Europhys. Lett. **97**, 17007 (2012).

[37] P. Calabrese, J. Cardy, and E. Tonni, J. Stat. Mech. (2013) P02008.

[38] P. Calabrese, L. Tagliacozzo, and E. Tonni, J. Stat. Mech. (2013) P05002.

[39] A. Coser, L. Tagliacozzo, and E. Tonni, J. Stat. Mech. (2014) P01008.

[40] C. De Nobili, A. Coser, and E. Tonni, J. Stat. Mech. (2015) P06021.

[41] P. Ruggiero, E. Tonni, and P. Calabrese, J. Stat. Mech. (2018) 113101.

[42] S. Singha Roy, S. N. Santalla, J. Rodríguez-Laguna, and G. Sierra, Phys. Rev. B **101**, 195134 (2020).

[43] G. Vidal, Phys. Rev. Lett. **91**, 147902 (2003).

[44] G. Vidal, Phys. Rev. Lett. **98**, 070201 (2007).

[45] Y. H. Su, S. Y. Cho, B. Li, H. L. Wang, and H. Q. Zhou, J. Phys. Soc. Jpn. **81**, 074003 (2012).

[46] J. Solyom and P. Pfeuty, Phys. Rev. B **24**, 218 (1981).

[47] F. Y. Wu, Rev. Mod. Phys. **54**, 235 (1982).

[48] R. J. Baxter, *Exactly Solved Models in Statistical Mechanics* (Academic Press, London, 1982).

[49] P. P. Martin, *Potts Models and Related Problems in Statistical Mechanics* (World Scientific, Singapore, 1991).

[50] Y.-H. Su, B.-Q. Hu, S.-H. Li, and S. Y. Cho, Phys. Rev. E **88**, 032110 (2013).

[51] Y.-W. Dai, S. Y. Cho, M. T. Batchelor, and H.-Q. Zhou, Phys. Rev. E **89**, 062142 (2014).

[52] C. Holzhey, F. Larsen, and F. Wilczek, Nucl. Phys. B **424**, 443 (1994).

[53] G. Vidal, J. I. Latorre, E. Rico, and A. Kitaev, Phys. Rev. Lett. **90**, 227902 (2003).

[54] J. I. Latorre, E. Rico, and G. Vidal, Quantum Inf. Comput. **4**, 048 (2004).

[55] B.-Q. Jin and V. E. Korepin, J. Stat. Phys. **116**, 79 (2004).

[56] V. E. Korepin, Phys. Rev. Lett. **92**, 096402 (2004)

[57] N. Laflorencie, E. S. Sørensen, M.-S. Chang, and I. Affleck, Phys. Rev. Lett. **96**, 100603 (2006).

[58] S. Ryu and T. Takayanagi, Phys. Rev. Lett. **96**, 181602 (2006).

[59] S. Ryu and T. Takayanagi, J. High Energy Phys. 08 (2006) 045.

[60] In this work, all the numerical fittings were performed by using the cftool function in the MATLAB Toolbox, which is archived by the principle of least squares. Details about numerical fittings with fitting errors are explained in https://www.mathworks.com/help/curvefit/curvefitting-app.html.

[61] E. Lieb, T. Schultz, and D. Mattis, Ann. Phys. **16**, 407 (1961).

[62] S. Katsura, Phys. Rev. **127**, 1508 (1962); **129**, 2835 (1963).

[63] E. Lieb and D. Mattis, *Mathematical Physics in One Dimension* (Academic Press, New York, London, 1966).

[64] P. Pfeuty, Ann. Phys. (NY) **57**, 79 (1970).

[65] K. Damle and S. Sachdev, Phys. Rev. Lett. **76**, 4412 (1996).

[66] J. E. Bunder and R. H. McKenzie, Phys. Rev. B **60**, 344 (1999).

[67] S.-A. Cheong and C. L. Henley, Phys. Rev. B **79**, 212402 (2009).

[68] K. V. Krutitsky, A. Osterloh, and R. Schützhold, Sci. Rep. **7**, 3634 (2017).